



Preoperative Radiological Evaluation

7

Burce Ozgen

7.1 Introduction

Cross-sectional imaging has become an indispensable tool in the preoperative assessment of cochlear implant (CI) and auditory brainstem implant (ABI) patients.

In infants and young children, computerized tomography (CT) and/or magnetic resonance (MR) imaging examinations of the inner ear are routinely performed to identify a potential etiology for hearing loss, to define the anatomy of the temporal bone and the auditory pathways, and for surgical planning [1]. In the setting of preoperative imaging, the evaluation of the cochlea and cochlear nerve determines the eligibility of the patient for the cochlear versus auditory brainstem implantation. Additionally, the imaging of the posterior fossa as well as supratentorial structures is crucial for appropriate preoperative assessment of a CI/ABI candidate.

7.2 Imaging Modalities

The ideal initial imaging modality for the evaluation of children with newly diagnosed SNHL is currently a topic of debate. Historically, CT has been the study of choice, but there is an increased

use of MR imaging due to concerns regarding the ionizing radiation exposure in small children who are more radiosensitive [2]. However dual-technique imaging (with CT and MR imaging) was found to identify a larger number of abnormalities in preimplant candidates than either technique alone [3]. CT and MR imaging are mostly complementary in the preoperative work-up, each with its own strengths and weaknesses [1, 4–9].

7.3 CT Imaging

CT enables accurate anatomical surgical planning, visualizing the bony structures of the ear and anatomical variants that may influence surgery such as facial nerve course or mastoid pneumatization [10]. Multidetector CT (MDCT) can be performed in a relatively short time without a need for sedation and at a lower cost.

CT of the temporal bone is able to delineate the detailed anatomy of the inner ear, but can also help to demonstrate anatomical variants that may influence surgery. The two currently available and recommended CT scanners for the imaging of the temporal bone are multidetector CT (MDCT) and cone-beam CT (CBCT).

7.3.1 MDCT

MDCT is the most commonly used and widely available method to evaluate the temporal bone

B. Ozgen (✉)
Department of Radiology, University of Illinois at Chicago, Chicago, IL, USA
e-mail: bozgen2@uic.edu

with CT. The image acquisition is performed in the axial plane; however, isotropic voxels allow reformatted images with high resolution in any additional plane. Scans have to extend from the top of the petrous apex to the mastoid tip in the axial direction with reformatted coronal images from the anterior tip of the petrous apex to the posterior margin of the mastoid. The imaging parameters are scanner specific but the collimation is usually chosen to be 0.5–0.625 mm and has to be less than 1 mm. Images should always be processed with a bone algorithm and viewed with a window width of 4000 HU and a window level of 200–500 HU [11].

7.3.2 CBCT

Although MDCT is used worldwide, CBCT using flat panel detector technology is slowly taking over for detailed evaluation of the small temporal bone structures [11]. The CBCT uses a rotating gantry and a cone-shaped X-ray beam that generates 3D volumetric dataset [11]. Newer cone-beam techniques offer higher resolution (0.15 mm thickness) but at lower radiation doses compared to traditional MDCT, making it valuable in the pediatric patient group. This technique is however more sensitive to motion as the acquisition usually lasts for 40 s and anesthesia may be required for small children.

For either technique, the CT of the temporal bone for the assessment of SNHL is routinely done without intravenous contrast.

7.4 MR Imaging

One of the main advantages of the MR imaging is the lack of ionizing radiation. However, due to longer exam times (of at least 20 min) the patient cooperation is paramount and anesthesia is usually required for small children. MR imaging has a higher soft tissue contrast compared to CT and is critical in the assessment of the cochlear nerve and also for a detailed evaluation of the auditory pathway [6, 8, 12–14]. Advances in MR imaging technology, including high-field-strength mag-

nets, improved coil technology, and new sequence designs, allow increasingly more detailed imaging of the inner ear [15–18].

MR imaging should be performed with a 3.0 Tesla scanner, whenever possible, as higher field strength improves the signal-to-noise ratio (SNR) and increases the spatial resolution [17]. MR imaging for the evaluation of an implant candidate should include high-resolution heavily T2-weighted (T2W) sequence for a detailed evaluation of the membranous labyrinth but especially for the assessment of the cochlear nerve.

These sequences can be achieved with both gradient-echo (GRE) and fast spin-echo (FSE) T2-weighted techniques but the choice of which sequence to prefer is a heavily debated and published topic [19]. The most commonly used and widely available sequences include constructive interference into steady state (CISS), fast imaging employing steady-state acquisition (FIESTA), driven equilibrium radio frequency reset pulse (DRIVE), 3D true-fast imaging with steady-state precession (FISP), 3D T2 FSE, or 3D T2 FSE with fast recovery (FRFSE) depending on the scanner vendor. A high resolution of these sequences should be obtained despite thin slice thickness (of less than 1 mm) with appropriate increased scanning time. Those high T2 weighted images (with a spatial resolution approaching 0.4 mm) enable detailed evaluation of very small cochlear structures such as the interscalar septum and lamina spiralis but more importantly allow for rigorous assessment of the neural structures. For the accurate assessment of the cochlear nerve sagittal oblique images are required and although reformatted images can be obtained in the sagittal oblique plane from the axial dataset, bilateral direct sagittal oblique images, perpendicular to the IACs, with the same heavily T2-weighted sequence should always be acquired as the direct sagittal oblique images have a better resolution than reformatted images [20]. The T2-weighted imaging of the entire brain is also required to assess the auditory pathway [21, 22].

Intravenous contrast is not routinely administered in children assessed for SNHL unless there is a clinical concern for underlying neoplasm or infectious/inflammatory cause of hearing loss.

7.5 Imaging Evaluation

7.5.1 CT Evaluation

The imaging evaluation of a child with congenital SNHL primarily focuses on the detection of possible inner ear anomaly. The imaging appearances of different types of inner ear anomalies are further detailed in respective chapters.

Probably the most important function of the CT evaluation is to detect contraindications for the cochlear implantation including cochlear aplasia but also aplasia of the cochlear nerve canal/cochlear aperture (Fig. 7.1).

The atresia of the cochlear aperture is a strong indicator of underlying cochlear nerve anomaly [23, 24]. Tahir et al. reported that all 21 cases with cochlear aperture atresia in their series had accompanying cochlear nerve deficiency (either aplasia or hypoplasia) [23]. The dimension of a patent cochlear aperture thus needs to be assessed, as its diameter is a marker of the cochlear nerve status [23, 25]. The cochlear aperture is considered stenotic when it is narrower than 1.4 mm (Fig. 7.2) [7, 26–29]. It is critical to realize that the aperture can be stenotic in the presence of a normal-appearing and normal-sized cochlea; thus, a normal cochlear shape does not always indicate normal cochlear nerve structure and further imaging with MR is required to assess the cochlear nerve status [23]. The internal auditory

canal size is also crucial for the preoperative assessment.

The IAC is considered stenotic when the diameter at its midpoint is smaller than 2 mm [30]. The IAC stenosis or atresia may easily be demonstrated by CT and the finding of a narrow or aplastic IAC again should raise concern for a deficiency of the cochlear nerve [24, 31]. However, the IAC morphology is an unreliable surrogate marker of CN integrity and as reported by Adunka et al., a normal IAC diameter can be

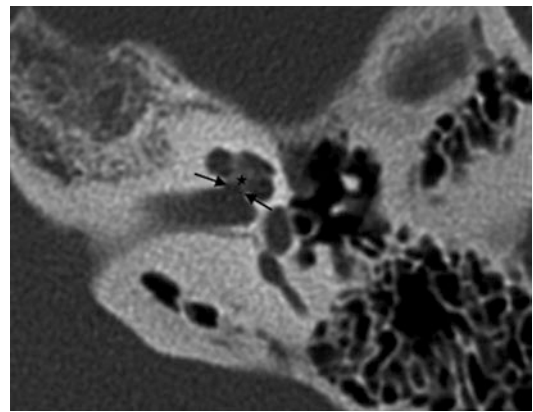


Fig. 7.1 CT anatomy of the cochlea. Axial temporal bone CT image demonstrates normal appearance of the cochlear aperture (delineated by the arrows). Note the normal appearance of the Modiolus (star) at the base of the cochlea

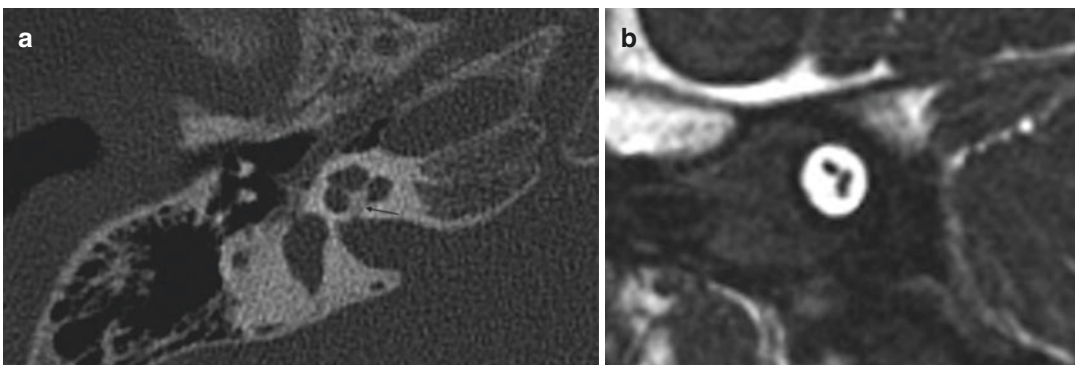


Fig. 7.2 Axial temporal bone CT (a) and sagittal oblique 3D-DRIVE image (b) of a patient with bilateral congenital severe SNHL. The CT image of the right ear reveals

atresia of the right cochlear aperture (arrow) with aplasia of the cochlear nerve on the corresponding MR image (b)

seen in up to half of cochlear nerve aplasia patients [23, 32].

During the imaging evaluation, the cochlea should be carefully assessed not only for possible malformations as the type and severity of the cochlear anomaly will determine the type of the implant used, but also for possible presence of labyrinthine ossificans (Fig. 7.3). Furthermore, CT may demonstrate anomalies of the bony labyrinth such as Paget and otosclerosis (Fig. 7.4) that could increase the incidence of postimplant complications such as facial nerve irritation.

Preoperative assessment should also detect entities that may increase the degree of surgical difficulty such as mastoid sclerosis, abnormal

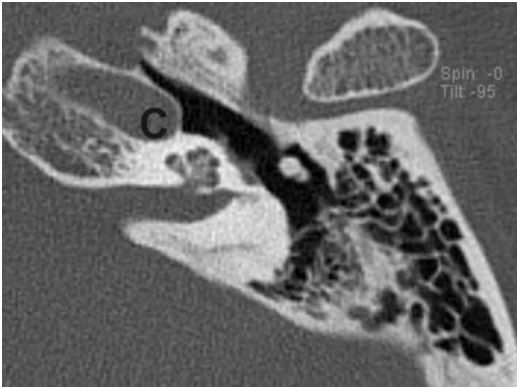


Fig. 7.3 Axial temporal bone CT revealing mineralization within the cochlea consistent with labyrinthine ossificans (c carotid canal)

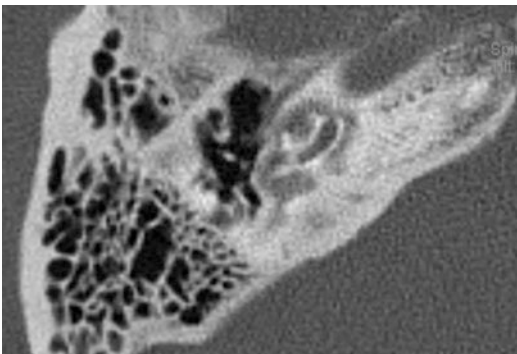


Fig. 7.4 Axial temporal bone CT revealing pericochlear lucency consistent with **extensive** retrofenestral otosclerosis

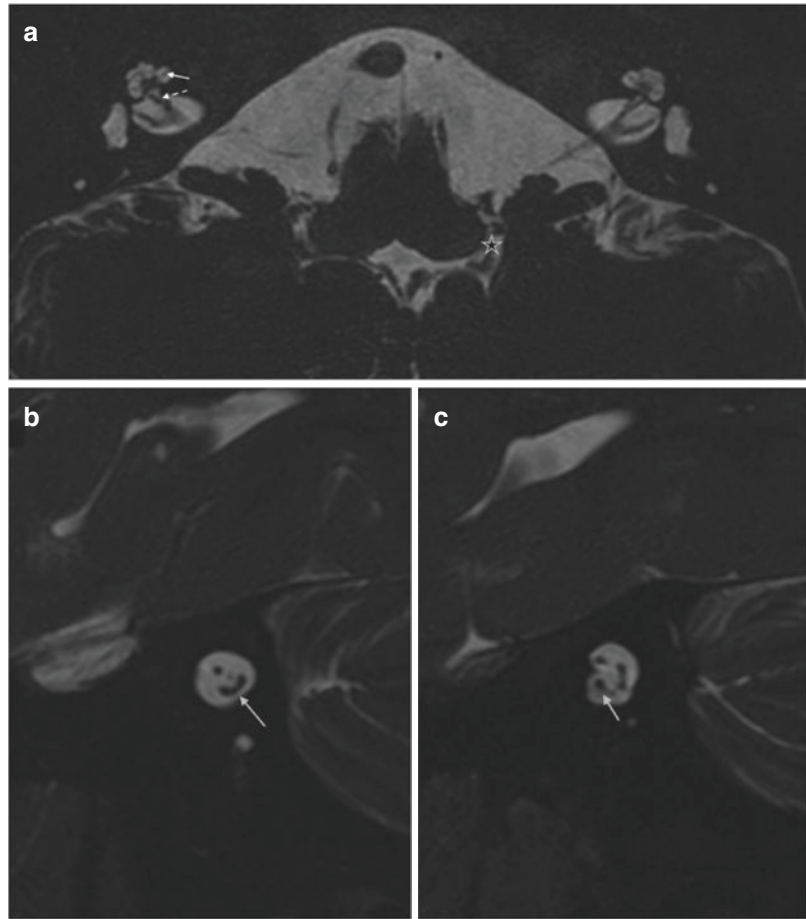
sigmoid sinus position, high riding jugular bulb, aberrant carotid artery, and especially dehiscent or aberrant facial nerve. The size of the round window should also be assessed as there might be congenital or acquired stenosis of the round window [33]. Additionally, the thickness of the bone at the potential pedestal placement and large emissary veins in that location should also be noticed and conveyed to the referring physician.

7.5.2 MR Imaging Evaluation

MRI with the heavily T2-weighted gradient-echo sequence allows a high spatial resolution that allows detailed visualization of the cochlear structures (Fig. 7.5a), allowing accurate depiction of the modiolum, lamina spiralis, and interscalar septum [34, 35].

Radiological assessment with MR not only gives detailed information regarding the inner ear structures but it is also essential for the assessment of the cochlear nerve. The evaluation of the cochleovestibular nerve and especially of its cochlear branch is of extreme importance prior to cochlear implantation. In a normal-sized IAC the diagnosis of cochlear nerve aplasia is relatively straightforward with dedicated sagittal oblique high-resolution images (Fig. 7.5b, c) [36]. However, in a very stenotic IAC, the diagnosis may be difficult because of the inability to separate the nerves [30, 32]. Again the visualized inner ear may be normal or have subtle abnormality despite severe deficiency of the cochlear nerve [12, 36]. Differentiation between hypoplasia and a normal size of the cochlear nerve can also be challenging and requires the highest possible resolution [12]. There is not a well-defined consensus regarding the definition of cochlear nerve hypoplasia. Li et al. defined cochlear nerve hypoplasia as a cochlear nerve with a diameter smaller than that of the facial nerve, seen on the oblique sagittal images. Similarly Glastonbury designated the cochlear nerve as small when it appeared decreased in size compared with the other nerves of the IAC [12]. It is critical to recognize that there might be

Fig. 7.5 Anatomy of the cochlea and cochlear nerve by high-resolution MR. Heavy T2-weighted driven equilibrium (DRIVE) images in axial (a) and sagittal oblique (b and c) planes. The cochlear turns with internal spiral lamina (arrow) are visible with this high T2-weighted axial image (a). The cochlear nerve (dotted arrow) is seen at the fundus of the IAC (a). With sagittal oblique imaging, the vestibulocochlear nerve (arrow) is seen as a crescent-shaped structure at the medial aspect of the IAC (b); however more laterally the cochlear nerve (arrow) can be seen separately from the inferior and superior vestibular nerves (c)



occasional discrepancy between the imaging and audiological findings regarding the presence/functionality of the cochlear nerve [37, 38]. Several studies have shown that subsets of patients with cochlear nerve aplasia have positive audiological responses and might derive benefit from cochlear implantation [37–39]. Anatomical connections between the cochlear nerve and other branches of the vestibulocochlear complex that are below the resolution of the current MR imaging might be responsible for this radiological-audiological inconsistency [40]. Imaging with ultra-high field magnets with DTI fiber tractography might solve this problem in the future [18, 41].

In every patient who is a candidate for a CI or ABI placement, the imaging of the brainstem and supratentorial brain structures with MRI is crucial to verify the integrity of the auditory path-

ways up to the temporal cortex but also to determine possible underlying congenital or acquired malformations that might hinder post-implant rehabilitation [42, 43].

MR imaging is better in delineating details of the brain anatomy but it is somewhat limited in the brainstem [44]. The difficulties in assessing the brainstem by using MR imaging arise not only from the small size of various brainstem structures but also from the fact that those anatomical components do not exhibit enough contrast to enable their individual identification [45]. Therefore, when relaxation-based MR image contrast is used, despite high resolution, conspicuity of those structures such as cranial nerve nuclei cannot be achieved in clinical field strengths [46]. Nevertheless, the bulge of the medulla into the lateral recess of the fourth ventricle and to the foramen of Luschka caused by

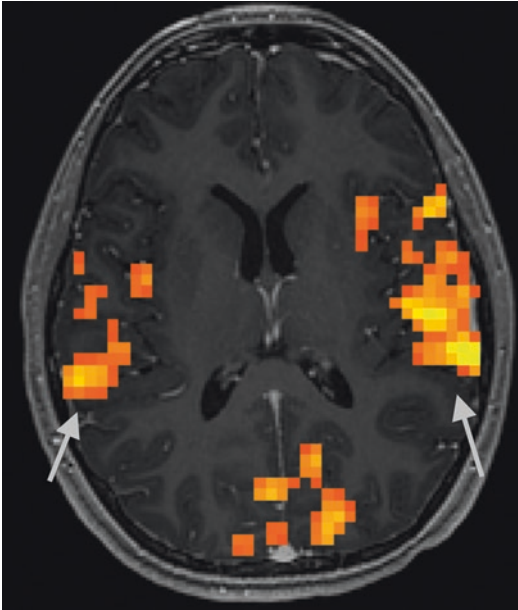


Fig. 7.6 Axial image from a BOLD fMRI study demonstrating bilateral activation of the auditory cortex (arrows). (Courtesy of Dr. Keith Thulborn)

the cochlear nuclear complex can be easily identified by MR imaging [47]. There is significant variability of the anatomy of the lateral recess in children with congenital deafness due to abnormalities of embryonic and fetal development [48].

It has been previously reported that congenital developmental abnormalities of the brain is more common in patients with auditory neuropathy spectrum disorder [1, 22, 48]. In patients with bilateral cochlear nerve deficiency hindbrain anomalies, such as pontine hypoplasia, were reported to be the most common abnormal intracranial finding [48]. Additionally there might be evidence of central pathologies such as chronic changes of hypoxic-ischemic injury, kernicterus, and chronic changes of congenital CNS infections [49, 50]. White matter lesions are also common findings in the preimplant imaging of the CI/ABI candidates [22, 51]. These lesions are nonspecific but more diffuse and prominent parenchymal changes were found to represent negative prognostic factors for speech and language development [21, 50, 51]. It is therefore critical to make a comprehensive evaluation of

the brainstem and cerebrum in each CI and ABI candidate.

Similar to the cochlear nuclear complex, the ascending fibers of the auditory pathway are not visible with normal visual inspection of routine MR sequences. The auditory radiation can only be demonstrated with dedicated fiber tracking obtained from diffusion tensor imaging [52]. With new developing technologies, MRI also has the potential to study the anatomical and functional organization of the auditory cortex through voxel-based morphometry and functional MRI (fMRI) (Fig. 7.6) [53]. DTI metrics, such as fractional anisotropy, may prove important in selecting patients and predicting outcomes after the implantation [54].

References

1. Joshi VM, Navlekar SK, Kishore GR, Reddy KJ, Kumar ECV. CT and MR imaging of the inner ear and brain in children with congenital sensorineural hearing loss. *Radiographics*. 2012;32(3):683–98. <https://doi.org/10.1148/rg.323115073>.
2. Brenner DJ, Hall EJ. Computed tomography—an increasing source of radiation exposure. *N Engl J Med*. 2007;357(22):2277–84. <https://doi.org/10.1056/NEJMr072149>.
3. Trimble K, Blaser S, James AL, Papsin BC. Computed tomography and/or magnetic resonance imaging before pediatric cochlear implantation? Developing an investigative strategy. *Otol Neurotol*. 2007;28(3):317–24. <https://doi.org/10.1097/01.mao.0000253285.40995.91>.
4. Lo WW. Imaging of cochlear and auditory brain stem implantation. *AJNR Am J Neuroradiol*. 1998;19(6):1147–54.
5. Marsot-Dupuch K, Meyer B. Cochlear implant assessment: imaging issues. *Eur J Radiol*. 2001;40(2):119–32.
6. Sennaroglu L, Saatci I, Aralasmak A, Gursel B, Turan E. Magnetic resonance imaging versus computed tomography in pre-operative evaluation of cochlear implant candidates with congenital hearing loss. *J Laryngol Otol*. 2002;116(10):804–10. <https://doi.org/10.1258/00222150260293619>.
7. Miyasaka M, Nosaka S, Morimoto N, Taiji H, Masaki H. CT and MR imaging for pediatric cochlear implantation: emphasis on the relationship between the cochlear nerve canal and the cochlear nerve. *Pediatr Radiol*. 2010;40(9):1509–16. <https://doi.org/10.1007/s00247-010-1609-7>.

8. Connor SE. Contemporary imaging of auditory implants. *Clin Radiol*. 2017;73(1):19–34. <https://doi.org/10.1016/j.crad.2017.03.002>.
9. Parry DA, Booth T, Roland PS. Advantages of magnetic resonance imaging over computed tomography in preoperative evaluation of pediatric cochlear implant candidates. *Otol Neurotol*. 2005;26(5):976–82.
10. Henderson E, Wilkins A, Huang L, Kenna M, Gopen Q. Histopathologic investigation of the dimensions of the cochlear nerve canal in normal temporal bones. *Int J Pediatr Otorhinolaryngol*. 2011;75(4):464–7. <https://doi.org/10.1016/j.ijporl.2010.11.024>.
11. Lemmerling M, de De Foer B. *Temporal bone imaging*. Berlin, Heidelberg: Springer; 2014.
12. Glastonbury CM, Davidson HC, Harnsberger HR, Butler J, Kertesz TR, Shelton C. Imaging findings of cochlear nerve deficiency. *AJNR Am J Neuroradiol*. 2002;23(4):635–43.
13. Russo EE, Manolidis S, Morriss MC. Cochlear nerve size evaluation in children with sensorineural hearing loss by high-resolution magnetic resonance imaging. *Am J Otolaryngol*. 2006;27(3):166–72. <https://doi.org/10.1016/j.amjoto.2005.09.007>.
14. Young NM, Rojas C, Deng J, Burrowes D, Ryan M. Magnetic resonance imaging of Cochlear implant recipients. *Otol Neurotol*. 2016;37(6):665–71. <https://doi.org/10.1097/MAO.0000000000001053>.
15. van Egmond SL, Visser F, Pameijer FA, Grolman W. Ex vivo and in vivo imaging of the inner ear at 7 tesla MRI. *Otol Neurotol*. 2014;35(4):725–9. <https://doi.org/10.1097/MAO.0000000000000276>.
16. van Egmond SL, Visser F, Pameijer FA, Grolman W. In vivo imaging of the inner ear at 7T MRI: image evaluation and comparison with 3T. *Otol Neurotol*. 2015;36(4):687–93. <https://doi.org/10.1097/MAO.0000000000000621>.
17. Schulze M, Reimann K, Seeger A, Klose U, Ernemann U, Hauser TK. Improvement in imaging common temporal bone pathologies at 3 T MRI: small structures benefit from a small field of view. *Clin Radiol*. 2017;72(3):267e261–12. <https://doi.org/10.1016/j.crad.2016.11.019>.
18. Thylur DS, Jacobs RE, Go JL, Toga AW, Niparko JK. Ultra-high-field magnetic resonance imaging of the human inner ear at 11.7 tesla. *Otol Neurotol*. 2017;38(1):133–8. <https://doi.org/10.1097/MAO.0000000000001242>.
19. Glastonbury C. The vestibulocochlear nerve, with an emphasis on the normal and diseased internal auditory canal and cerebellopontine angle. In: *Imaging of the temporal bone*. New York, NY: Thieme Medical; 2009. p. 480–558.
20. Noij KS, Remenschneider AK, Kozin ED, Puram S, Herrmann B, Cohen M, Cunnane MB, Lee DJ. Direct parasagittal magnetic resonance imaging of the internal auditory canal to determine cochlear or auditory brainstem implant candidacy in children. *Laryngoscope*. 2015;125(10):2382–5. <https://doi.org/10.1002/lary.25228>.
21. Moon IJ, Kim EY, Park GY, Jang MS, Kim JH, Lee J, Chung WH, Cho YS, Hong SH. The clinical significance of preoperative brain magnetic resonance imaging in pediatric cochlear implant recipients. *Audiol Neurootol*. 2012;17(6):373–80. <https://doi.org/10.1159/000341818>.
22. Lapointe A, Viamonte C, Morriss MC, Manolidis S. Central nervous system findings by magnetic resonance in children with profound sensorineural hearing loss. *Int J Pediatr Otorhinolaryngol*. 2006;70(5):863–8. <https://doi.org/10.1016/j.ijporl.2005.09.022>.
23. Tahir E, Bajin MD, Atay G, Mocan BO, Sennaroglu L. Bony cochlear nerve canal and internal auditory canal measures predict cochlear nerve status. *J Laryngol Otol*. 2017;131(8):676–83. <https://doi.org/10.1017/S0022215117001141>.
24. Li Y, Yang J, Liu J, Wu H. Restudy of malformations of the internal auditory meatus, cochlear nerve canal and cochlear nerve. *Eur Arch Otorhinolaryngol*. 2015;272(7):1587–96. <https://doi.org/10.1007/s00405-014-2951-4>.
25. Fatterpekar GM, Mukherji SK, Alley J, Lin Y, Castillo M. Hypoplasia of the bony canal for the cochlear nerve in patients with congenital sensorineural hearing loss: initial observations. *Radiology*. 2000;215(1):243–6. <https://doi.org/10.1148/radiology.215.1.r00ap36243>.
26. D'Arco F, Talenti G, Lakshmanan R, Stephenson K, Siddiqui A, Carney O. Do measurements of inner ear structures help in the diagnosis of inner ear malformations? A review of literature. *Otol Neurotol*. 2017;38(10):e384–92. <https://doi.org/10.1097/mao.0000000000001604>.
27. Lan M-Y, Shiao J-Y, Ho C-Y, Hung H-C. Measurements of normal inner ear on computed tomography in children with congenital sensorineural hearing loss. *Eur Arch Otorhinolaryngol*. 2009;266(9):1361–4. <https://doi.org/10.1007/s00405-009-0923-x>.
28. Stjernholm C, Muren C. Dimensions of the cochlear nerve canal: a radioanatomic investigation. *Acta Otolaryngol*. 2002;122(1):43–8.
29. Yi JS, Lim HW, Kang BC, Park S-Y, Park HJ, Lee K-S. Proportion of bony cochlear nerve canal anomalies in unilateral sensorineural hearing loss in children. *Int J Pediatr Otorhinolaryngol*. 2013;77(4):530–3. <https://doi.org/10.1016/j.ijporl.2012.12.031>.
30. Romo LV, Casselman JW, Robson CD. Temporal bone: congenital anomalies. In: Som PM, Curtin HD, editors. *Head and neck imaging*. 5th ed. St. Louis, MO: Elsevier Health Sciences; 2011. p. 1097–165.
31. Shelton C, Luxford WM, Tonokawa LL, Lo WW, House WF. The narrow internal auditory canal in children: a contraindication to cochlear implants. *Otolaryngol Head Neck Surg*. 1989;100(3):227–31. <https://doi.org/10.1177/019459988910000310>.
32. Adunka OF, Roush PA, Teagle HFB, Brown CJ, Zdanski CJ, Jewells V, Buchman CA. Internal auditory canal morphology in children with Cochlear nerve deficiency. *Otol Neurotol*. 2006;27(6):793–801. <https://doi.org/10.1097/01.mao.0000227895.34915.94>.

33. Monsanto RC, Sennaroglu L, Uchiyama M, Sancak IG, Paparella MM, Cureoglu S. Histopathology of inner ear malformations: potential pitfalls for Cochlear implantation. *Otol Neurotol*. 2019;40(8):e839–46. <https://doi.org/10.1097/mao.0000000000002356>.
34. Reinshagen KL, Curtin HD, Quesnel AM, Juliano AF. Measurement for detection of incomplete partition type II anomalies on MR imaging. *Am J Neuroradiol*. 2017;38(10):2003–7. <https://doi.org/10.3174/ajnr.A5335>.
35. Davidson HC, Harnsberger HR, Lemmerling MM, Mancuso AA, White DK, Tong KA, Dahlen RT, Shelton C. MR evaluation of vestibulocochlear anomalies associated with large endolymphatic duct and sac. *Am J Neuroradiol*. 1999;20(8):1435–41.
36. Casselman JW, Offeciers FE, Govaerts PJ, Kuhweide R, Geldof H, Somers T, D'Hont G. Aplasia and hypoplasia of the vestibulocochlear nerve: diagnosis with MR imaging. *Radiology*. 1997;202(3):773–81. <https://doi.org/10.1148/radiology.202.3.9051033>.
37. Peng KA, Kuan EC, Hagan S, Wilkinson EP, Miller ME. Cochlear nerve aplasia and hypoplasia: predictors of Cochlear implant success. *Otolaryngol Head Neck Surg*. 2017;157(3):392–400. <https://doi.org/10.1177/0194599817718798>.
38. Young NM, Kim FM, Ryan ME, Tournis E, Yaras S. Pediatric cochlear implantation of children with eighth nerve deficiency. *Int J Pediatr Otorhinolaryngol*. 2012;76(10):1442–8. <https://doi.org/10.1016/j.ijporl.2012.06.019>.
39. Acker T, Mathur NN, Savy L, Graham JM. Is there a functioning vestibulocochlear nerve? Cochlear implantation in a child with symmetrical auditory findings but asymmetric imaging. *Int J Pediatr Otorhinolaryngol*. 2001;57(2):171–6. [https://doi.org/10.1016/S0165-5876\(00\)00458-4](https://doi.org/10.1016/S0165-5876(00)00458-4).
40. Ozdogmus O, Sezen O, Kubilay U, Saka E, Duman U, San T, Cavdar S. Connections between the facial, vestibular and cochlear nerve bundles within the internal auditory canal. *J Anat*. 2004;205(1):65–75. <https://doi.org/10.1111/j.0021-8782.2004.00313.x>.
41. Vos SB, Haakma W, Versnel H, Froeling M, Speleman L, Dik P, Viergever MA, Leemans A, Grolman W. Diffusion tensor imaging of the auditory nerve in patients with long-term single-sided deafness. *Hear Res*. 2015;323:1–8. <https://doi.org/10.1016/j.heares.2015.01.010>.
42. Sennaroglu L, Ziyal I. Auditory brainstem implantation. *Auris Nasus Larynx*. 2012;39(5):439–50. <https://doi.org/10.1016/j.anl.2011.10.013>.
43. Colletti G, Mandala M, Colletti L, Colletti V. Nervus intermedius guides auditory brainstem implant surgery in children with Cochlear nerve deficiency. *Otolaryngol Head Neck Surg*. 2016;154(2):335–42. <https://doi.org/10.1177/0194599815615858>.
44. Sclocco R, Beissner F, Bianciardi M, Polimeni JR, Napadow V. Challenges and opportunities for brainstem neuroimaging with ultrahigh field MRI. *Neuroimage*. 2018;168:412–26. <https://doi.org/10.1016/j.neuroimage.2017.02.052>.
45. Beissner F. Functional MRI of the brainstem: common problems and their solutions. *Clin Neuroradiol*. 2015;25(Suppl 2):251–7. <https://doi.org/10.1007/s00062-015-0404-0>.
46. Lambert C, Lutti A, Helms G, Frackowiak R, Ashburner J. Multiparametric brainstem segmentation using a modified multivariate mixture of Gaussians. *Neuroimage Clin*. 2013;2:684–94. <https://doi.org/10.1016/j.nicl.2013.04.017>.
47. Gebarski SS, Tucci DL, Telian SA. The cochlear nuclear complex: MR location and abnormalities. *AJNR Am J Neuroradiol*. 1993;14(6):1311–8.
48. Huang BY, Roche JP, Buchman CA, Castillo M. Brain stem and inner ear abnormalities in children with auditory neuropathy spectrum disorder and cochlear nerve deficiency. *AJNR Am J Neuroradiol*. 2010;31(10):1972–9. <https://doi.org/10.3174/ajnr.A2178>.
49. Jallu AS, Jehangir M, Ul Hamid W, Pampori RA. Imaging evaluation of pediatric sensorineural hearing loss in potential candidates for Cochlear implantation. *Indian J Otolaryngol Head Neck Surg*. 2015;67(4):341–6. <https://doi.org/10.1007/s12070-015-0819-6>.
50. Xu XQ, Wu FY, Hu H, Su GY, Shen J. Incidence of brain abnormalities detected on preoperative brain MR imaging and their effect on the outcome of Cochlear implantation in children with sensorineural hearing loss. *Int J Biomed Imaging*. 2015;2015:275786. <https://doi.org/10.1155/2015/275786>.
51. Hong P, Jurkowski ZC, Carvalho DS. Preoperative cerebral magnetic resonance imaging and white matter changes in pediatric cochlear implant recipients. *Int J Pediatr Otorhinolaryngol*. 2010;74(6):658–60. <https://doi.org/10.1016/j.ijporl.2010.03.014>.
52. Javad F, Warren JD, Micallef C, Thornton JS, Golay X, Yousry T, Mancini L. Auditory tracts identified with combined fMRI and diffusion tractography. *Neuroimage*. 2014;84:562–74. <https://doi.org/10.1016/j.neuroimage.2013.09.007>.
53. Semenza C, Cavinato M, Rigon J, Battel I, Meneghello F, Venneri A. Persistent cortical deafness: a voxel-based morphometry and tractography study. *Neuropsychology*. 2012;26(6):675–83. <https://doi.org/10.1037/a0029688>.
54. Huang L, Zheng W, Wu C, Wei X, Wu X, Wang Y, Zheng H. Diffusion tensor imaging of the auditory neural pathway for clinical outcome of Cochlear implantation in pediatric congenital sensorineural hearing loss patients. *PLoS One*. 2015;10(10):e0140643. <https://doi.org/10.1371/journal.pone.0140643>.